International Journal of Fracture **108:** 119–131, 2001.

Variation of stress intensity factor along the front of a 3D rectangular crack by using a singular integral equation method

QING WANG, NAO-AKI NODA, MASA-AKI HONDA and MENGCHENG CHEN
Department of Mechanical Engineering, Kyushu Institute of Technology, Kitakyushu 804-8550, Japan
(Author for correspondence; e-mail: noda@mech.kyutech.ac.jp)

Received 15 March 2000; accepted in revised form 30 August 2000

Abstract. In this paper a singular integral equation method is applied to calculate the distribution of stress intensity factor along the crack front of a 3D rectangular crack. The stress field induced by a body force doublet in an infinite body is used as the fundamental solution. Then, the problem is formulated as an integral equation with a singularity of the form of r^{-3}. In solving the integral equation, the unknown functions of body force densities are approximated by the product of a polynomial and a fundamental density function, which expresses stress singularity along the crack front in an infinite body. The calculation shows that the present method gives smooth variations of stress intensity factors along the crack front for various aspect ratios. The present method gives rapidly converging numerical results and highly satisfied boundary conditions throughout the crack boundary.

Key words: Body force method, elasticity, fundamental density function, numerical solution, polynomial, rectangular crack, singular integral equation, stress intensity factor.

Nomenclature:
a, b = half width of a rectangular crack, area = the area of defects or cracks projected in the direction of the maximum principal stress, $(\xi, \psi, \zeta) = (x, y, z)$ coordinate where a body force doublet is applied, $f(\xi, \eta) =$ density of body force doublet, u_z = displacement in the z direction, E = Young's modulus, $H = (1 - 2\nu)/4(1 - \nu)^2$, $R(\theta)$ = a distance between a point (x, y) and a point on the prospective boundary of crack, $U_z(x, y)$ = crack opening displacement, ν = Poisson's ratio.

1. Introduction

Three dimensional crack solutions have been used to evaluate the strength of structures because they usually contain some defects in the form of cracks, voids, inclusions or second-phase particles. The fatigue limit of structural materials including defects is not the critical stress below which no cracks appear around the defects, but the threshold stress where a fatigue crack, which developed under the stress level around the defects, stops propagating. In this sense an arbitrary shaped defect sometimes should be evaluated as a crack having the same projected area of the defect. From this viewpoint Murakami et al. have proposed convenient formulas useful for evaluating arbitrary shaped cracks with less than 10% estimated error. The formula gives the maximum stress intensity factor appearing at a certain point along the crack front in the following equations.

For surface cracks (Murakami and Nemat-Nasser, 1983; Murakami, 1985)

$$K_I \max = 0.65\sigma\sqrt{\pi\sqrt{\text{area}}}. \tag{1}$$

For internal cracks (Murakami and Endo, 1983; Murakami et al., 1988)

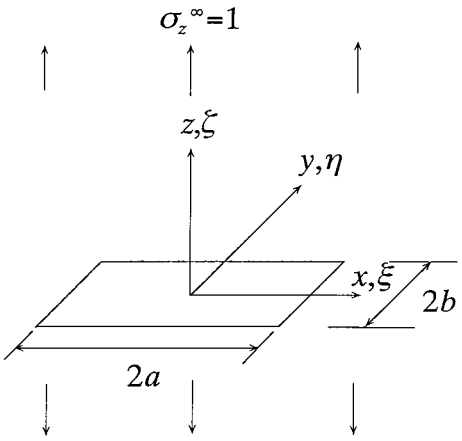

Figure 1. A rectangular crack in a infinite body.

$$K_I \max = 0.50\sigma\sqrt{\pi\sqrt{\text{area}}}, \tag{2}$$

where 'area' is the area of defects or crack projected in the direction of the maximum principal stress. Recently, Equation (1) is found to estimate the maximum stress intensity factor of a semi-elliptical crack with less than 3% error (Noda and Miyoshi; 1996). Equation (2) is based on the exact solution of an elliptical crack; however, it is necessary to evaluate the error when Equation (2) is applied to different shape of ellipse because sometimes the shape of defects are very different from ellipse.

From this viewpoint, this paper deals with a rectangular crack as a shape different from ellipse. There are some studies about a rectangular crack made by Weaver (1977), Mastrojannis et al. (1979), Kassir (1981, 1982), Abe et al. (1982), Isida et al. (1982, 1983, 1991), and Murakami and Nemat-Nasser (1983). However, the variation of the stress intensity factor along the crack front has not been indicated and also there is little discussion about the accuracy of the results. For example, Isida et al. (1991) indicated that those previous results are different about 4.8% on the average and 7.5% at the most.

In this analysis the problem is formulated as an integral equation with a singularity of the form of r^{-3}. In solving the integral equation, the unknown functions of body force densities are approximated by the product of a polynomial and a fundamental density function. In the previous papers boundary conditions are found to be satisfied within the error of 3×10^{-3} throughout the crack surfaces (Noda-Miyoshi, 1995; Noda et al., 1999). Then, it will be shown that the smooth variations of stress intensity factor along the crack front and highly satisfactory boundary conditions throughout the crack surface.

2. Singular integral equation of the body force method

Consider an infinite body having a rectangular crack as shown in Figure 1 which is subjected to uniform tension σ_z^x at $|z| \to \infty$.

On the idea of the body force method (Nisitani, 1967; Nisitani and Murakami, 1974), the problem is reduced to determining the density of force doublet $f(\xi, \eta)$, which is distributed on the prospective boundary for crack in an infinite body without a crack.

$$\begin{aligned}
&\frac{H}{2\pi}\iint \frac{f(\xi,\eta)}{r_1^3}\mathrm{d}\xi\ \mathrm{d}\eta = -\sigma_z^x,\\
&r_1 = \sqrt{(x-\xi)^2+(y-\eta)^2}, \quad H(1-2\nu)/4(1-\nu)^2,\\
&S = \left\{(\xi,\eta)\middle| -a \leqslant \xi \leqslant a, -b \leqslant \eta \leqslant b\right\},
\end{aligned} \tag{3a}$$

$$U_z(x,y) = u_z(x,y,+0) - u_z(x,y,-0) = \frac{(1-2v)(1+v)}{E(1-v)} f(x,y). \tag{3b}$$

The force doublet density (ξ,η) directly gives the crack opening displacement by Equation (3b). Equation (3) enforces the boundary condition at the imaginary boundary of a crack; that is $\sigma_z = 0$. The integral in Equation (3) should be interpreted as a finite part integral (Hadamard, 1923) in the region S.

3. Numerical solution of singular integral equations

In the present analysis, polynomials have been used to approximate the unknown functions as a continuous function. First, we put

$$\begin{aligned}
f(\xi,\eta) &= F(\xi,\eta)w(\xi,\eta),\\
w(\xi,\eta) &= \frac{\sigma_z^\infty}{H}\sqrt{a^2-\xi^2}\sqrt{b^2-\eta^2}.
\end{aligned} \tag{4}$$

Then, the integral Equation (3) becomes

$$\frac{1}{2\pi}\left[\iint \frac{F(\xi,\eta)}{r_1^3}\sqrt{a^2-\xi^2}\sqrt{b^2-\eta^2}\ \mathrm{d}\xi\ \mathrm{d}\eta\right] = -1. \tag{5}$$

Here, $F(\xi,\eta)$ is now approximated in terms of polynomials as follows.

$$\begin{aligned}
F(\xi,\eta) = {} & \alpha_0 + \alpha_1\eta^{2\times1} + \cdots + \alpha_{n-1}\eta^{2(n-1)} + \alpha_n\eta^{2n}\\
&+\alpha_{n+1}\xi^{2\times1} + \alpha_{n+2}\xi^{2\times1}\eta^{2\times1} + \cdots + \alpha_{2n}\xi^{2\times1}\eta^{2n}\\
&+\alpha_{l-n-1}\xi^{2n} + \alpha_{l-n}\xi^{2n}\eta^{2\times1} + \cdots + \alpha_{l-1}\xi^{2n}\eta^{2n}\\
= {} & \sum_{i=0}^{l}\alpha_i G_i(\xi,\eta), \quad l = (n+1)(n+1)\\
G_0(\xi,\eta) = {} & 1, G_1(\xi,\eta) = \eta^{2\times1}, \cdots,\\
&G_{n+1}(\xi,\eta) = \xi^{2\times1}, \ldots, G_{l-1}(\xi,\eta) = \xi^{2n}\eta^{2n}
\end{aligned} \tag{6a}$$

$$\begin{aligned}
\xi^{2n} &= x^{2n} + 2nx^{2n-1}(\xi-x) + \sum_{i=0}^{2n-2}\left\{(i+1)\xi^{(2n-2-i)}x^i\right\}(\xi-x)^2\\
&= b_0(x) + b_1(x)(\xi-x) + b_2(\xi,x)(\xi-x)^2\\
\eta^{2n} &= y^{2n} + 2ny^{2n-1}(\eta-y) + \sum_{i=0}^{2n-2}\left\{(i+1)\eta^{(2n-2-i)}y^i\right\}(\eta-y)^2\\
&= c_0(y) + c_1(y)(\eta-y) + c_2(\eta,y)(\eta-y)^2
\end{aligned} \tag{6b}$$

Using the approximation method mentioned above, we obtain the following system of linear equations for the determination of the coefficients $\alpha_i [i = 0, 1, 2, \ldots, (n+1)(n+1)]$. The unknown coefficients α_i are then determined from (7a) by selecting a set of collocation points.

$$\frac{1}{2\pi}\sum_{i=0}^{l}\alpha_i A_i = -1, \tag{7a}$$

$$A_i = \iint \frac{G_i(\xi,\eta)}{r_1^3}\sqrt{a^2-\xi^2}\sqrt{b^2-\eta^2}\,\mathrm{d}\xi\,\mathrm{d}\eta \tag{7b}$$

4. How to evaluate hypersingular integrals

In (7b), the integral A_i has a hypersingularity of the form r^{-3} when $x = \xi$ and $y = \eta$; therefore, in order to evaluate A_i the following expressions will be used (Noda and Miyoshi, 1995).

$$\begin{aligned}
F_1 &= \sqrt{a^2-\xi^2} = \sqrt{a^2-x^2} + \sqrt{a^2-\xi^2} - \sqrt{a^2-x^2} \\
&= \sqrt{a^2-x^2} + \frac{a^2-\xi^2-(a^2-x^2)}{\sqrt{a^2-\xi^2}+\sqrt{a^2-x^2}} \\
&= \sqrt{a^2-x^2} - (\xi-x)\frac{\xi+x}{\sqrt{a^2-\xi^2}+\sqrt{a^2-x^2}} \\
&= \sqrt{a^2-x^2} - G(\xi-x),
\end{aligned}$$

$$\begin{aligned}
G &= \frac{\xi+x}{\sqrt{a^2-\xi^2}+\sqrt{a^2-x^2}} \\
&= \frac{x}{\sqrt{a^2-x^2}} + \frac{\xi+x}{\sqrt{a^2-\xi^2}+\sqrt{a^2-x^2}} - \frac{x}{\sqrt{a^2-x^2}} \\
&= \frac{x}{\sqrt{a^2-x^2}} + \frac{\sqrt{a^2-x^2}\,(\xi+x) - x\left(\sqrt{a^2-\xi^2}+\sqrt{a^2-x^2}\right)}{\sqrt{a^2-x^2}\left(\sqrt{a^2-\xi^2}+\sqrt{a^2-x^2}\right)} \\
&= \frac{x}{\sqrt{a^2-x^2}} + \frac{\xi\sqrt{a^2-x^2} - x\sqrt{a^2-\xi^2}}{\sqrt{a^2-x^2}\left(\sqrt{a^2-\xi^2}+\sqrt{a^2-x^2}\right)} \\
&= \frac{x}{\sqrt{a^2-x^2}} + \frac{\xi^2\left(a^2-x^2\right) - x^2\left(a^2-\xi^2\right)}{\sqrt{a^2-x^2}\left(\sqrt{a^2-\xi^2}+\sqrt{a^2-x^2}\right)} \\
&\quad \times \frac{1}{\left(\sqrt{a^2-x^2}+x\sqrt{a^2-\xi^2}\right)} \\
&= \frac{x}{\sqrt{a^2-x^2}} + (\xi-x)\frac{\xi+x}{\sqrt{a^2-x^2}\left(\sqrt{a^2-\xi^2}+\sqrt{a^2-x^2}\right)} \\
&\quad \times \frac{1}{\left(\xi\sqrt{a^2-x^2}+x\sqrt{a^2-\xi^2}\right)}.
\end{aligned} \tag{8a}$$

$$
\begin{aligned}
\therefore F_1 = {} & \sqrt{a^2-x^2} - (\xi - x)\frac{x}{\sqrt{a^2-x^2}} \\
& -(\xi - x)^2 \frac{\xi + x}{\sqrt{a^2-x^2}\left(\sqrt{a^2-\xi^2}+\sqrt{a^2-x^2}\right)} \\
& \times \frac{1}{\left(\xi\sqrt{a^2-x^2}+x\sqrt{a^2-\xi^2}\right)}, \\
F_2 = {} & \sqrt{b^2-y^2} - (\eta - y)\frac{y}{\sqrt{b^2-y^2}} \\
& -(\eta - y)^2 \frac{\eta - y)}{\sqrt{b^2-y^2}\left(\sqrt{b^2-\eta^2}+\sqrt{b^2-y^2}\right)} \\
& \times \frac{1}{\left(\eta\sqrt{b^2-y^2}+y\sqrt{b^2-\eta^2}\right)},
\end{aligned}
$$

$$
\begin{aligned}
& F_1 = P_0(x) - (\xi - x)P_1(x) - (\xi - x)^2 P_2(\xi, x), \\
& F_2 = Q_0(y) - (\eta - y)Q_1(y) - (\eta - y)^2 Q_2(\eta, y), \\
& P_0(x) = \sqrt{a^2-x^2},\ Q_0(y) = \sqrt{b^2-y^2},
\end{aligned}
\tag{8b}
$$

$$
\begin{aligned}
P_1(x) = {} & \frac{x}{\sqrt{a^2-x^2}},\ P_2(\xi, x) = \frac{\xi + x}{\sqrt{a^2-x^2}\left(\sqrt{a^2-\xi^2}+\sqrt{a^2-x^2}\right)} \\
& \times \frac{a^2}{\left(\xi\sqrt{a^2-y^2}+x\sqrt{a^2-\xi^2}\right)}, \\
Q_1(y) = {} & \frac{y}{\sqrt{b^2-y^2}},\ Q_2(\eta, y) = \frac{\eta + y}{\sqrt{b^2-y^2}\left(\sqrt{b^2-\eta^2}+\sqrt{b^2-y^2}\right)} \\
& \times \frac{b^2}{\left(\eta\sqrt{b^2-y^2}+y\sqrt{b^2-\eta^2}\right)},
\end{aligned}
$$

$$
\begin{aligned}
F_1F_2 = {} & P_0Q_0(\eta - y)P_0Q_1 - (\eta - y)^2 P_0Q_2 \\
& -(\xi - x)P_1Q_0 + (\xi - x)\eta - y)P_1Q_1 \\
& +(\xi - x)(\eta - y)^2 P_1Q_2 - (\xi - x)^2 P_2Q_0 \\
& +(\xi - x)^2(\eta - y)P_2Q_1 + (\xi - x)^2(\eta - y)^2 P_2Q_2.
\end{aligned}
\tag{8c}
$$

In Equation (8), it should be noted that $P_0(x)$, $P_1(x)$, $Q_0(y)$, $Q_1(y)$, $b_0(x)$, $b_1(x)$, $c_0(y)$, $c_1(y)$ are independent of ξ, η. By using a polar coordinate and the relations $(\xi - x) = r\cos\theta$, $(\eta - y) = r\sin\theta$ shown in Figure 2, Equation (8) becomes

$$
\begin{aligned}
& \sqrt{a^2-\xi^2}\sqrt{b^2-\eta^2} = A_0 + A_1(\theta)r + A_2(r,\theta)r^2, \\
& \xi^{2n} = B_{0i} + B_{1i}(\theta)r + B_{2i}(r,\theta)r^2, \\
& \eta^{2n} = C_{0i} + C_{1i}(\theta)r + C_{2i}(r,\theta)r^2,
\end{aligned}
\tag{9}
$$

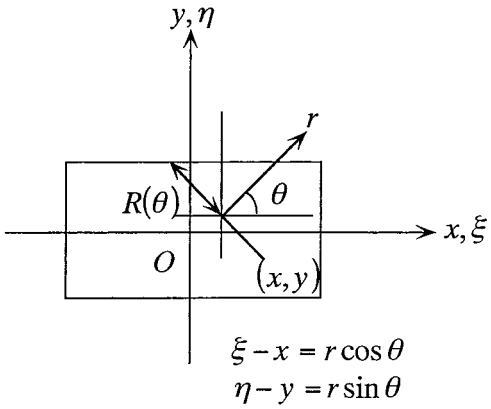

Figure 2. Change of integral parameter from (ξ, η) to (x, y).

$$
\begin{aligned}
A_0 &= P_0(x)Q_0(y),\\
A_1 &= -P_0(x)Q_1(y)\ \sin\theta - P_1(x)Q_0(y)\ \cos\theta,\\
A_2 &= -P_2(\xi, x)Q_0(y)\ \cos^2\theta + P_1(x)Q_1(y)\ \sin\theta\ \cos\theta\\
&\quad -P_0(x)Q_2(\eta, y)\ \sin^2\theta + P_1(x)Q_2\ (\eta, y)\ \cos\theta\ \sin^2\theta\\
&\quad +P_2(\xi, x)Q_1(y)\ \cos^2\theta\ \sin\theta + P_2(\xi, x)Q_2(eta, y)\ \cos^2\theta, \sin^2\theta,\\
B_0 &= b_0(x),\\
B_1(\theta) &= b_1(x)\ \cos\theta,\\
B_2(r, \theta) &= b_2(\xi, x)\ \cos^2\theta,\\
C_0 &= c_0(y),\\
C_1(\theta) &= c_1(y)\ \sin\theta,\\
C_2(r, \theta) &= c_2(\eta, y)\ \sin^2\theta,
\end{aligned}
\tag{10}
$$

Then, we can also obtain the expression

$$
\begin{aligned}
G_i(\xi, \eta)\sqrt{a^2 - \xi^2}\sqrt{b^2 - \eta^2} = {} & D_{0i} + D_{1i}(\theta \cdot r + D_{2i}(r, \theta) \cdot r^2\\
& + D_{3i}(r, \theta) \cdot r^3 + D_{4i}(r, \theta) \cdot r^4\\
& + D_{5i}(r, \theta) \cdot r^5 + D_{6i}(r, \theta) \cdot r^6
\end{aligned}
\tag{11a}
$$

where

$$
\begin{aligned}
D_{0i} &= A_0 \cdot B_0 \cdot C_0,\\
D_{1i}(\theta) &= A_0 \cdot B_0 \cdot C_1 + A_0 \cdot B_1 \cdot C_0 + A_1 \cdot B_0 \cdot C_0,\\
D_{2i}(r, \theta) &= A_0 \cdot B_0 \cdot C_2 + A_0 \cdot B_2 \cdot C_0 + A_2 \cdot B_0 \cdot C_0\\
&\quad + A_0 \cdot B_1 \cdot C_1 + A_1 \cdot B_0 \cdot C_1 + A_1 \cdot B_1 \cdot C_0,\\
D_{3i}(r, \theta) &= A_0 \cdot B_1 \cdot C_2 + A_1 \cdot B_0 \cdot C_2 + A_0 \cdot B_2 \cdot C_1\\
&\quad + A_1 \cdot B_2 \cdot C_0 + A_2 \cdot B_0 \cdot C_1 + A_2 \cdot B_1 \cdot C_0 + A_1 \cdot B_1 \cdot C_1,\\
D_{4i}(r, \theta) &= A_0 \cdot B_2 \cdot C_2 + A_1 \cdot B_1 \cdot C_2 + A_2 \cdot B_0 \cdot C_2\\
&\quad + A_1 \cdot B_2 \cdot C_1 + A_2 \cdot B_2 \cdot C_0 + A_2 \cdot B_1 \cdot C_1,
\end{aligned}
\tag{11b}
$$

$$D_{5i}(r,\theta) = A_2 \cdot B_2 \cdot C_2 + A_2 \cdot B_1 \cdot C_2 + A_2 \cdot B_2 \cdot C_1,$$
$$D_{6i}(r,\theta) = A_2 \cdot B_2 \cdot C_2.$$

By substituting (11) into (7b), we obtain

$$\begin{aligned} A_i &= \int_0^{2\pi}\int_0^{R(\theta)} \left[\frac{D_{0i}}{r^2} + \frac{D_{1i}(\theta)}{r}\right] \mathrm{d}r\ \mathrm{d}\theta \\ &\quad + \int_0^{2\pi}\int_0^{R(\theta)} \left[D_{2i}(r,\theta) + D_{3i}(r,\theta)r + D_{4i}(r,\theta)r^2 + D_{5i}(r,\theta)r^3 \right. \\ &\quad \left. + D_{6i}(r,\theta)r^4\right] \mathrm{d}r\ \mathrm{d}\theta \\ &= A_{ai} + A_{bi}. \end{aligned} \tag{12}$$

Here, A_{bi} has no singularities and can be evaluated easily in numerical integration. On the other hand, A_{ai} has singularities; however, they are expressed simply in the form r^{-1} or r^{-2}, so they can be evaluated in a Hadamard sense as shown in (13).

$$A_{ai} = \int_0^{2\pi} \left[-\frac{D_{0i}}{R(\theta)} + D_{1i}(\theta)\ \log\left(R(\theta)\right)\right] \mathrm{d}\theta. \tag{13}$$

Here, $R(\theta)$ means a distance between a point (x, y) and a point on the prospective boundary of crack as shown in Figure 2.

5. Numerical results and discussion

Numerical integrals have been performed using scientific subroutine library (FACOM SOL2 AQME etc.). In demonstrating the numerical results of stress intensity factor (SIF), the following dimensionless factor F_I will be used. Here, F_I is expressed on the basis of the SIF of a 2D crack whose length is $2b$.

$$F_I = \frac{K_I\,(x, y)\,\big|_{x=x,\,y=\pm b}}{\sigma_z^{\infty}\sqrt{\pi b}} = \sqrt{a^2 - x^2}\,F\,(x, y)\,\big|_{x=x,\,y=\pm b}. \tag{14}$$

In this analysis, it is important to evaluate the integrals as shown in Equation (7b) accurately. Figure 3 shows the values of integral $A_i/2\pi$ in (7b) when $G_i(\xi,\eta) = 1$, $G_i(\xi,\eta) = \eta^2$, $G_i(\xi,\eta) = \xi^2\eta^2$ for $b/a = 1$. In this analysis, the boundary condition for crack surface $\sigma_z = -1$ will be satisfied by superposing those smooth functions as indicated in Figure 3. Here, the rectangular shape is mapped into a $a \times a$ square; then, the boundary conditions are considered at the intersection of the $m \times m$ mesh as shown in Figure 4. In solving the algebraic Equation (5) the least square method is applied to minimize the residual of stress at the collocation points.

Tables 1–3 show the convergence of dimensionless stress intensity factors F_I along the crack front with increasing parameter n when $b/a = 1.0$, 0.25. As shown in Tables 1 and 2, number of collocation points 10×10 are large enough because the results of 10×10 coincide with the ones of 30×30 to the third digit in most cases. Figure 4 indicate the compliance of the boundary conditions along the prospective crack surface with varying n in Equation (6). The boundary condition becomes highly satisfied with increasing n and when n=7 and collocation points 10×10 the error is less than 2×10^{-4}.

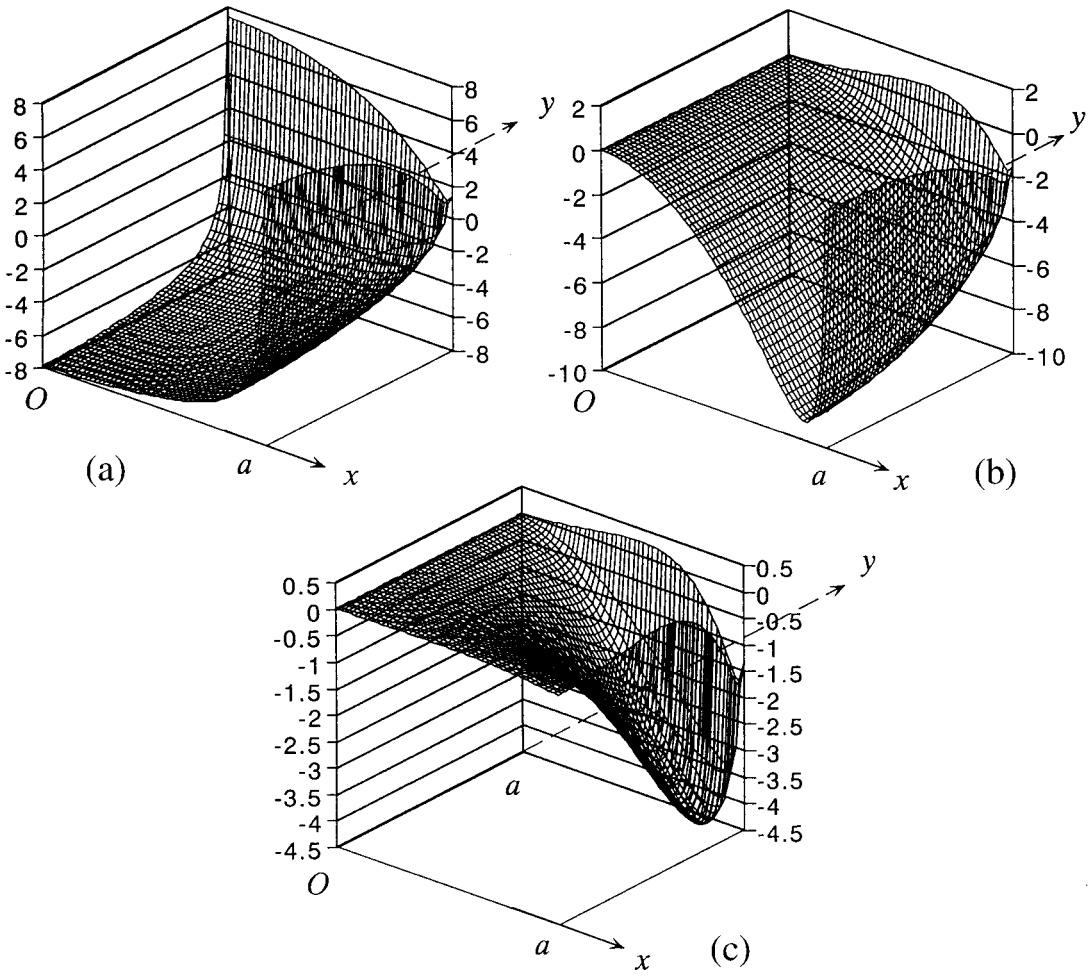

Figure 3. Numerical values of Equation (6). (a) $G_i(\xi, \eta) = 1$, (b) $G_i(\xi, \eta) = \eta^2$, (c) $G_i(\xi, \eta) = \xi^2\eta^2$.

Table 1. Convergence of the results $F_I(b/a = 1.0$, number of collocation points $10 \times 10)$.

$\frac{x/a}{n}$	0/11	1/11	2/11	3/11	4/11	5/11	6/11	7/11	8/11	9/11	10/11	11/11
2	0.74652	0.74550	0.74228	0.73629	0.72651	0.71141	0.68865	0.65473	0.60403	0.52640	0.39793	0.00000
3	0.75652	0.75434	0.74788	0.73738	0.72305	0.70489	0.68221	0.65287	0.61184	0.54765	0.43045	0.00000
4	0.75235	0.75091	0.74636	0.73807	0.72522	0.70696	0.68254	0.65101	0.60980	0.55053	0.44384	0.00000
5	0.75375	0.75192	0.74645	0.73736	0.72436	0.70668	0.68293	0.65125	0.60908	0.55031	0.44973	0.00000
6	0.75336	0.75168	0.74654	0.73761	0.72448	0.70653	0.68273	0.65118	0.60879	0.54979	0.45253	0.00000
7	0.75341	0.75171	0.74652	0.73759	0.72450	0.70658	0.68277	0.65118	0.60859	0.54924	0.45361	0.00000

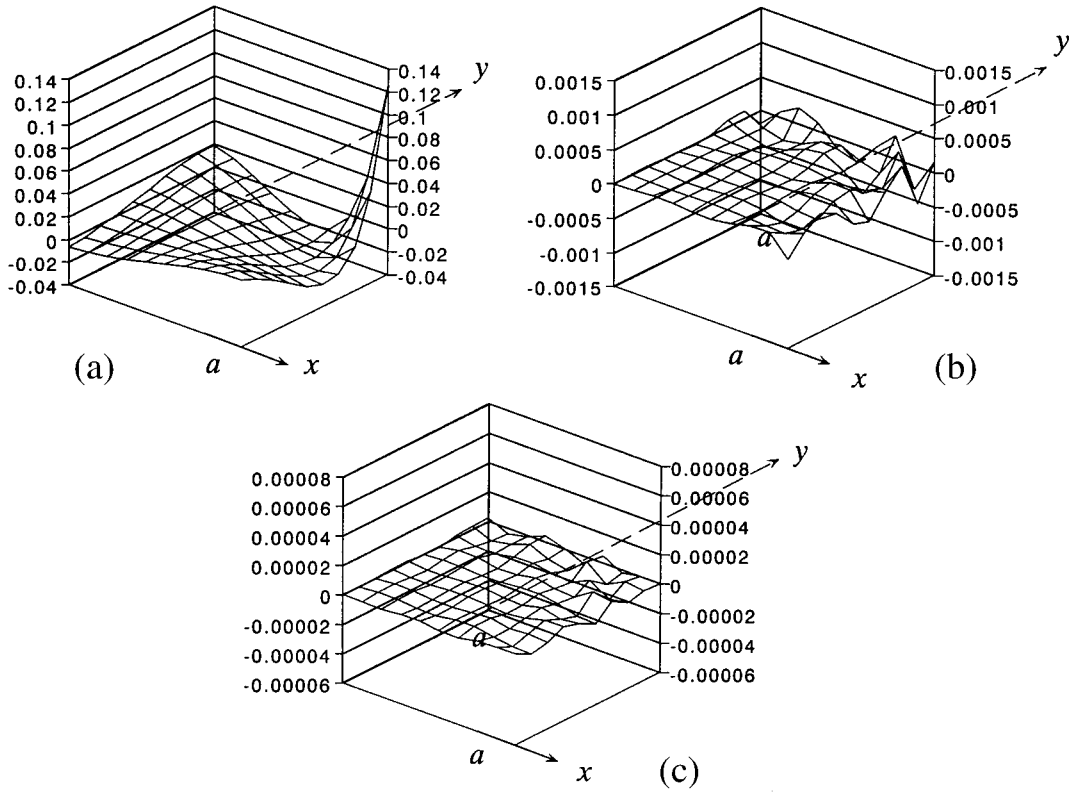

Figure 4. Compliance of boundary condition. (a) $n = 2, b/a = 1.0$; (b) $n = 5, b/a = 1.0$; (c) $n = 7, b/a = 1.0$.

Table 2. Convergence of the results $F_I(b/a = 1.0$, number of collocation points $30 \times 30)$.

$\frac{x/a}{n}$	0/31	3/31	6/31	9/31	12/31	15/31	18/31	21/31	24/31	27/31	30/31	31/31
2	0.74452	0.74358	0.74051	0.73455	0.72432	0.70768	0.68134	0.64013	0.57516	0.46790	0.25220	0.00000
3	0.75824	0.75541	0.74712	0.73394	0.71658	0.69544	0.66982	0.63655	0.58693	0.49824	0.28514	0.00000
4	0.75101	0.74981	0.74569	0.73721	0.72260	0.70042	0.67006	0.63135	0.58150	0.50368	0.30470	0.00000
5	0.75469	0.75218	0.74508	0.73423	0.71984	0.70044	0.67286	0.63343	0.57935	0.50197	0.31638	0.00000
6	0.75277	0.75124	0.74602	0.73589	0.72017	0.69898	0.67167	0.63442	0.58027	0.50017	0.32335	0.00000
7	0.75378	0.75157	0.74530	0.73528	0.72068	0.69975	0.67126	0.63372	0.58092	0.49957	0.32756	0.00000

Table 3. Convergence of the results $F_I(b/a = 0.25$, number of collocation points $10 \times 10)$.

$\frac{x/a}{n}$	0/11	1/11	2/11	3/11	4/11	5/11	6/11	7/11	8/11	9/11	10/11	11/11
2	0.94553	0.94739	0.95260	0.95995	0.96732	0.97147	0.96764	0.94879	0.90396	0.81399	0.63574	0.00000
3	0.98570	0.98355	0.97748	0.96842	0.95765	0.94621	0.93402	0.91831	0.89071	0.83059	0.68344	0.00000
4	0.97351	0.97365	0.97351	0.97164	0.96618	0.95543	0.93835	0.91422	0.88034	0.82481	0.69573	0.00000
5	0.97759	0.97654	0.97364	0.96930	0.96347	0.95485	0.94070	0.91726	0.88014	0.82052	0.69865	0.00000
6	0.97626	0.97576	0.97395	0.97018	0.96380	0.95418	0.93994	0.91768	0.88113	0.81975	0.69956	0.00000
7	0.97681	0.97602	0.97375	0.96993	0.96395	0.95449	0.93985	0.91741	0.88144	0.81973	0.70014	0.00000

Table 4. Dimensionless stress intensity factors F_I along crack front in Figure 1 ($n = 7$).

$\frac{x/a}{b/a}$	0/11 (Isida:[8])	1/11	2/11	3/11	4/11	5/11	6/11	7/11	8/11	9/11	10/11	11/11
8.000	0.290 (–)	0.289	0.287	0.283	0.277	0.268	0.257	0.241	0.219	0.189	0.141	0.000
4.000	0.405 (–)	0.404	0.401	0.396	0.389	0.380	0.367	0.349	0.323	0.285	0.220	0.000
2.000	0.566 (–)	0.564	0.560	0.553	0.542	0.528	0.510	0.486	0.454	0.409	0.328	0.000
1.000	0.753 (0.756)	0.752	0.747	0.738	0.725	0.707	0.683	0.651	0.609	0.549	0.453	0.000
0.667	0.852 (–)	0.850	0.848	0.836	0.823	0.804	0.779	0.746	0.700	0.634	0.525	0.000
0.500	0.906 (0.907)	0.904	0.900	0.892	0.879	0.862	0.839	0.806	0.760	0.692	0.576	0.000
0.250	0.977 (0.977)	0.976	0.974	0.970	0.964	0.954	0.940	0.917	0.881	0.820	0.699	0.000
0.125	0.995 (0.995)	0.995	0.995	0.994	0.992	0.989	0.985	0.976	0.959	0.920	0.820	0.000

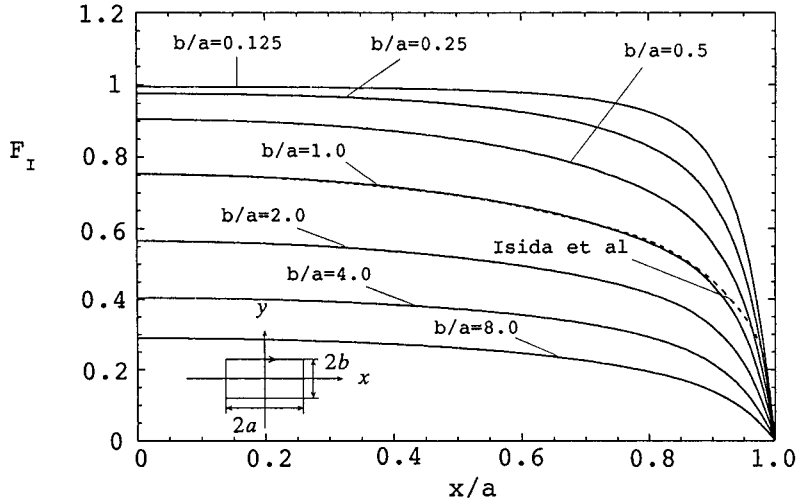

Figure 5. Variation of dimensionless stress intensity factors along the crack front $y = b$.

Table 4 and Figure 5 show the variation of F_I along the crack front when $b/a = 8.0$–0.125. In Figure 5, Isida's results for $b/a = 1$ are in close agreement with the present results; however there is a difference near $x/a = 1$. As shown in Figure 6, there are some differences about the maximum SIF of a rectangular crack obtained by Isida et al. (1991), Kassir (1983), Weaver (1977), and Mastrojannis et al. (1979). The difference is 4.8% on the average and 7.5% at the most. However, Isida's results are found to be more reliable because they are in close agreement with the present results within 0.4% error.

In Table 5 the accuracy of Murakami's formula (2) for arbitrary shaped crack is examined. Table 5 indicates that Murakami's formula gives approximate maximum values of stress intensity factor for rectangular cracks within 8% error, and for elliptical cracks within 5% error.

6. Conclusion

(1) A singular integral equation method was applied to calculate the stress intensity factor of a rectangular crack. The problem was formulated as an integral equation on the idea of the body force method. The unknown functions were approximated by the product of a funda-

Table 5. Maximum stress intensity factors $F_{I\,\max}$ of elliptical and rectangular cracks and the accuracy of Murakami's formula. [$F^*_{I\,\max} = \frac{K_{I\,\max}}{\sigma_z^\infty \sqrt{\pi \sqrt{\text{area}}}}$, $\delta = (F^*_{I\,\max} - 0.50) \times 100/F^*_{I\,\max}$, *when $b/a \leqslant 0.2$ area $= 20b^2$]. (a) Rectangular crack, (b) elliptical crack.

b/a	$F_{I\,\max}$	$F^*_{I\,\max}$	δ (%)
1.000	0.753	0.5325	+6.1
0.667	0.852	0.5444	+8.2
0.500	0.906	0.5387	+7.2
0.250	0.977	0.4885	−2.4
0.125	0.995	0.4705**	−6.3

b/a	a/b	$F_{I\,\max}$	$F^*_{I\,\max}$	δ (%)
1.00	1.00	0.6366	0.4782	−4.6
0.75	1.33	0.7240	0.5061	+1.2
0.50	2.00	0.8257	0.5215	+4.1
0.25	4.00	0.9330	0.4955	−0.9

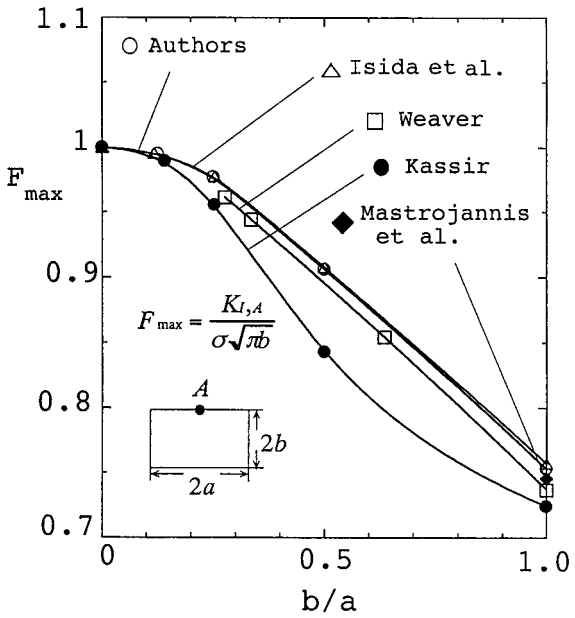

Figure 6. $F_{I\,\max}$ vs. b/a for a rectangular crack in an infinite body.

mental density function and a weight function. The calculation shows the method yields good convergence and highly satisfactory boundary condition and also smooth variations of stress intensity factor along the crack front.

(2) There are some differences among the previous results of the maximum SIF of a rectangular crack, about 4.8% on the average and 7.5% at the most. However, Isida's results coincide with the present results within 0.4% error.

(3) Murakami's formula (2) proposed for estimating arbitrary shaped cracks is found to give maximum stress intensity factors of a rectangular crack within 8% error, and an elliptical crack within 5% error.

Acknowledgement

The authors wish to express their thanks to the Japan Society for the Promotion of Science Postdoctoral Fellowship and Kyushu Institute of Technology Fellowship for Foreign Researchers.

References

Abe, H., Hayashi, K. and Enokida, Y. (1982). Stress intensity factors for a rectangular crack in a semi-infinite solids. *Trans. Japan Soc. Mech. Engrs* **48**, 29–34.

Hadamard, J. (1923). *Lectures on Caunchy's Problem in Linear Partial Differential Equations*, Yale University Press.

Isida, M., Yoshida, T. and Noguchi, H. (1982). A rectangular crack in an infinite solid, a semi-infinite solid and a finite-thickness plate subjected to tension. *Prelim Proc. Japan Soc. Mech. Engrs. and Japan Soc. Precision Engng., Mie District*, No. 823–3, pp. 15–17 (in Japanese).

Isida, M., Tsuru, H. and Noguchi, H. (1983). New method of analysis of three-dimensional crack problems. *Memoirs of the Faculty of Engineering, Kyushu University*, Vol. 43, No.4, pp. 317–334.

Isida, M., Yoshida, T. and Noguchi, H. (1991). A rectangular crack in an infinite solid, a semi-infinite solid and a finite-thickness plate subjected to tension. *International Journal of Fractures* **52**, 79–90.

Kassir, M.K. (1981). Stress intensity factor for a three-dimensional rectangular crack. *Trans. ASME, Sea. E* **48**, 309–312.

Kassir, M.K. (1982). A three-dimensional rectangular crack subjected to shear loading. *International Journal Solid and Structures* **18**, 1075–1082.

Mastrojannis, E.N., Keer, L.M. and Mura, T.A. (1979). "Stress Intensity Factor for a Plane Crack under Normal Pressure", *International Journal of Fractures* **15**, 247–258.

Murakami, Y. (1985). Analysis of stress intensity factors of Modes I, II and III inclined surface cracks of arbitrary shape. *Engng. Frac. Mech.* **22**, 101–114.

Murakami, Y. and Endo, M. (1983). Quantitative evaluation of fatigue strength of metals containing various small defects or cracks. *Engng. Frac. Mech.* **17**, 1–15.

Murakami, Y. and Nemat-Nasser, S. (1983). Growth and stability of interacting surface flaws of arbitrary shape. *Engng. Frac. Mech.* **17**, 193–210.

Murakami, Y., Kodama, S. and Konuma, S. (1988). Quantitative evaluation of effects of nonmetallic inclusions on fatigue strength of high strength steel. *Trans. Japan Society of Mechanical Engineers* **54**, 688–696 (in Japanese).

Nisitani, H. (1967). The two-dimensional stress problem solved using an electric digital computer. *Journal of the Japan Society of Mechanical Engineers* **70**, 627–632 (in Japanese).

Nisitani, H. (1968). *Bulletin of Japan Society of Mechanical Engineers* **11**, 14–23.

Nisitani, H. and Murakami, Y. (1974). Stress Intensity Factor of an Elliptical Crack and Semi-Elliptical Crack in Plates Subjected to Tension, *International Journal of Fractures* **10**, 353–368.

Noda, N.-A. and Miyoshi, S. (1996). Variation of stress intensity factor and crack opening displacement of a semi-elliptical surface crack. *International Journal of Fractures* **75**, 19–48.

Noda, N.-A., Kobayashi, K. and Yagishita, M. (1999). Variation of mixed modes stress intensity factors of an inclined semi-elliptical surface crack, *International Journal of Fractures* (in press).

Weaver, J. (1977). Three-Dimensional crack analysis. *International Journal of Solids Structures* **13**, 321–330.